



# Magnetic parameters in giant magnetoresistance spin valve and their roles in magnetoresistance sensitivity



Ku Hoon Chung, Si Nyeon Kim, Sang Ho Lim\*

Department of Materials Science and Engineering, Korea University, Seoul 02841, Republic of Korea

## ARTICLE INFO

### Keywords:

Giant magnetoresistance sensor  
Magnetic parameters  
Magnetoresistance sensitivity  
Interlayer coupling field

## ABSTRACT

Giant magnetoresistance (GMR) spin valves are fabricated and their  $m(H)$  ( $m$  and  $H$  are the magnetic moment and applied magnetic field, respectively) and  $MR(H)$  ( $MR$  is the magnetoresistance) curves are characterized, from which various magnetic parameters including the interlayer coupling field, the anisotropy field of the free and pinned layers, and the exchange bias field of the pinned layer are extracted. A more accurate exchange bias field is obtained by utilizing an analytical equation for the total energy describing the GMR spin valve. The exchange bias field is found to be greater than the bias of the pinned layer magnetization switching obtained from the experimental  $m(H)$  loops, with the difference being proportional to the product of the interlayer coupling field and the free layer magnetization. Among the magnetic parameters, the interlayer coupling field is the dominant factor affecting the sensitivity, which is the most important parameter in sensor applications. The anisotropy field of the free layer is the next important parameter in affecting the sensitivity, but its role is significantly less dominant, being only 15% of the role by the interlayer coupling field.

## 1. Introduction

The signal-to-noise ratio (SNR) is among the most important parameters in sensor applications. Among many types of magnetic sensors, giant magnetoresistance (GMR) spin-valve (SV) sensors are known to exhibit a high SNR and therefore have attracted significant attention [1–3]. There are two types of GMR SV sensors, depending on the direction of the applied current; current-in-plane (CIP) and current-perpendicular-to-plane (CPP). Although the magnetoresistance (MR) ratio is usually higher in the CPP configuration than in the CIP configuration, CIP SV sensors, which are the subject of this study, have several advantages of easy and simple device fabrication and high resistance (and hence high output voltage at a given current) over CPP ones [4]. In GMR SVs, the SNR has usually been correlated with the coercivity and bias field of the free layer [5], both of which can be obtained from  $m(H)$  loops ( $m$  and  $H$  are the magnetic moment and applied magnetic field, respectively) along the in-plane easy direction. These two parameters, however, should be of limited value in sensor applications where  $m(H)$  loops along the in-plane hard direction showing the absence of hysteresis and good linearity are more relevant than those along the in-plane easy direction. The main aim of the present study is to extract various magnetic parameters from  $m(H)$  loops and evaluate their roles in sensor applications. Both experimental and theoretical studies are performed.

## 2. Experimental and calculation methods

### 2.1. Experimental method

GMR SVs were deposited using an ultrahigh vacuum magnetron sputtering unit on the Si (111) substrate with lateral dimensions of  $10\text{ mm} \times 10\text{ mm}$ . The Si substrates were cleaned with an ultrasonic cleaner in acetone for 15 min and then in methanol for 15 min, followed by washing with deionized water. Two different stacks with the following structures were fabricated (the numbers in parentheses denote the layer thickness in nm):

(Sample I)

Si(SiOx)/Ta(5)/FeZr(2.5)/NiFe(3.5)/CoFe(2)/Cu(2.2)/CoFe(2)/IrMn(8)/Ta(5)

(Sample II)

Si(SiOx)/Ta(5)/FeZr(2.5)/Pd(4)/IrMn(8)/CoFe(2)/Cu(2.2)/CoFe(1.2)/NiFe(2.5)/CoFe(1.2)/Cu(2.2)/CoFe(2)/IrMn(8)/Ta(5)

For the alloys, the targets with the following compositions (in at.%) were used:  $\text{Fe}_{50}\text{Zr}_{50}$ ,  $\text{Ni}_{80}\text{Fe}_{20}$ ,  $\text{Co}_{90}\text{Fe}_{10}$ , and  $\text{Ir}_{21}\text{Mn}_{79}$ . The base pressure of the chamber was  $9.3 \times 10^{-6}$  Pa, and the Ar pressure during the deposition was 0.27 Pa. The power levels used to deposit the layers

\* Corresponding author.

E-mail address: [sangholim@korea.ac.kr](mailto:sangholim@korea.ac.kr) (S.H. Lim).

were 15 W for Ta and FeZr; 10 W for NiFe and CoFe; and 5 W for Cu, IrMn, and Pd. To form an induced anisotropy of the magnetic layers, an in-plane  $H$  value of 6.37 kA/m was applied during the deposition using ferrite magnets. As-deposited samples were annealed in a vacuum of  $6.7 \times 10^{-4}$  Pa at 250 °C for 10 min under an  $H$  value of 159.2 kA/m, the direction of which was identical to that of the induced anisotropy.  $m(H)$  loops were measured using a vibrating sample magnetometer along the in-plane easy and hard directions.  $MR(H)$  curves along the two directions were measured using the four-point probe method at a constant applied current of 1 mA.

## 2.2. Calculation method

In the Stoner–Wohlfarth (S-W) model, the total energy per unit area ( $E_{\text{tot}}$ ) for the GMR SVs can be expressed as follows:

$$E_{\text{tot}} = \frac{1}{2}\mu_0 H_{k,f} M_f t_f \sin^2 \alpha + \frac{1}{2}\mu_0 H_{k,p} M_p t_p \sin^2 \beta - \mu_0 H_{\text{ex}} M_p t_p \cos \beta - \mu_0 H_{\text{int}} M_f t_f \cos(\beta - \alpha) - \mu_0 H M_f t_f \cos(\theta - \alpha) - \mu_0 H M_p t_p \cos(\theta - \beta) \quad (1)$$

where  $\mu_0$  is the permeability of free space,  $H_k$  is the anisotropy field,  $M$  is the magnetization,  $t$  is the layer thickness,  $H_{\text{ex}}$  is the exchange bias field of the pinned layer,  $H_{\text{int}}$  is the interlayer coupling field (bias field of the free layer switching loop) between the free and pinned layers.  $\theta$ ,  $\alpha$ , and  $\beta$  are the angles between  $H_{\text{ex}}$  and  $H$ ,  $H_{\text{ex}}$  and  $M_f$ , and  $H_{\text{ex}}$  and  $M_p$ , respectively (refer to Fig. 1 for the orientations and angles used to set up Eq. (1)). The subscripts  $f$  and  $p$  denote the related properties of the free and pinned layers, respectively.  $H_{\text{int}}$  consists of the orange peel coupling field and Ruderman-Kittel-Kasuya-Yosida interactions. The  $H_{k,f}$  value was obtained from the experimental  $m(H)$  loops measured along the in-plane hard direction, where magnetization occurs mainly by magnetization rotation so that Eq. (1) based on the S-W model should be valid. To obtain a more accurate value of  $H_{k,f}$ , a separate stack containing the free magnetic layer only (viz., Ta(5)/FeZr(2.5)/NiFe(3.5)/CoFe(2)/Ta(5)), rather than the entire GMR stack, was used. The  $H_{\text{int}}$  value was extracted from the bias of the free layer, with respect to the origin, in the  $m(H)$  loops along the easy direction.  $H_{\text{ex}}$  could similarly be extracted from the bias of the pinned layer. However, it was found that when the  $H_{\text{ex}}$  value extracted in this way was used as the

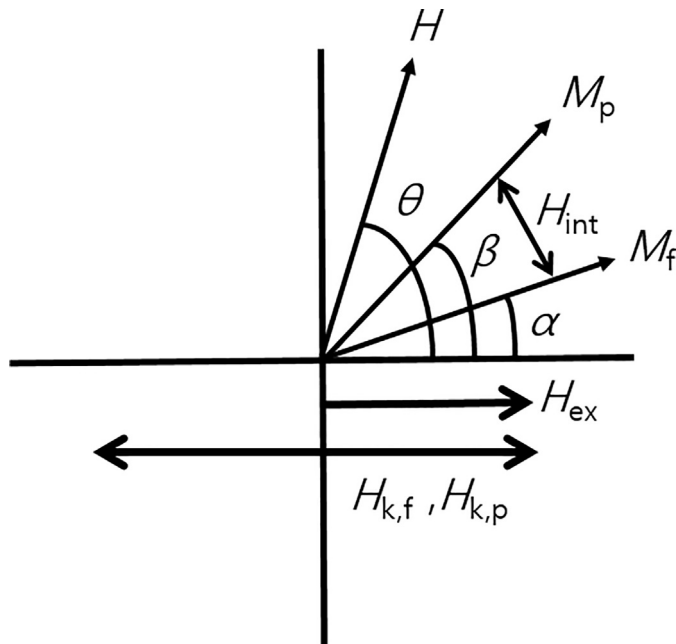


Fig. 1. Schematic diagram showing orientations and angles of model system used to set up Eq. (1). The direction is easy (hard) when the  $\theta$  value is 0° (90°).

input parameter in Eq. (1), the agreement between the experimental and calculated  $m(H)$  loops was rather poor. This was because of the coupling between the free and pinned layers through the interlayer coupling field. The interlayer coupling field, which usually prefers parallel coupling between free and pinned layers, will make the pinned layer switching harder when the two layers are parallel. On the other hand, when the two layers are antiparallel, the interlayer coupling field will facilitate the switching of the pinned layer. This means that the actual or intrinsic value of  $H_{\text{ex}}$ , caused by the antiferromagnetic pinning layer (IrMn), is different from the bias of the pinned layer. An accurate value of  $H_{\text{ex}}$  was then obtained by fitting the experimental  $m(H)$  loop with that calculated by Eq. (1). The  $m(H)$  loop along the easy direction was used in this fitting procedure. Considering that the S-W model is valid only when the magnetization occurs by magnetization rotation, not by domain-wall motion, an error may arise with the use of the loop along the easy direction. This error, however, is considered to be not large because a layer exchange-coupled by a pinning layer nearly follows a coherent magnetization behavior [6]. With the same reasoning, the  $H_{k,p}$  value was also extracted from the easy axis  $m(H)$  loop. Armed with these parameters, it is a straightforward task to calculate the  $H$  dependences of the resistance ( $R$ ) and MR, because both  $R$  and MR depend solely on the angle between the free and pinned layer magnetization directions [7]. The detailed equations for  $R$  and MR are as follows:

$$R(H) = R_p + \frac{R_{\text{ap}} - R_p}{2}(1 - \cos(\theta_f - \theta_p)) \quad (2)$$

$$\text{MR}(\%) = \frac{\text{MR}_{\text{max}}}{2}(1 - \cos(\theta_f - \theta_p)) \quad (3)$$

where  $R_p$  and  $R_{\text{ap}}$  are the resistances when the free and pinned layer magnetizations are parallel and antiparallel, respectively, and  $\text{MR}_{\text{max}}$  is the maximum MR ratio given by the relation  $(R_{\text{ap}} - R_p)/R_p$  and can be obtained from an easy axis MR curve.

## 3. Results and discussion

Fig. 2(a) and (b) show the  $m(H)$  curves of Sample I measured along the in-plane easy and hard directions, respectively, from which most of the magnetic parameters used in Eq. (1) can be extracted. The parameters of  $H_{\text{int}}$  and  $H_{k,p}$  were obtained from the easy-axis hysteresis loop (Fig. 2(a)): specifically, the former from the bias of the free layer switching loop (0.99 kA/m) and the latter from half the width of the pinned layer switching loop (7.16 kA/m). The  $H_{k,f}$  value could be determined from the hard-axis curve of the whole stack (Fig. 2(b)), but it was obtained accurately from an independent stack composed of only the free layer, the  $m(H)$  curves of which are shown in Fig. 2(c) measured along both directions. The  $H_{k,f}$  value is the saturation field in the hard-axis curve (1.4 kA/m), indicated by an arrow in Fig. 2(c). One remaining parameter of  $H_{\text{ex}}$  can usually be obtained from the bias of the pinned layer switching loop of the easy-axis curve (Fig. 2(a)), which is 41 kA/m. Armed with these parameters, it is a straightforward task to calculate the  $m(H)$  curves using Eq. (1), which are also shown in Fig. 2(a) and (b). The agreement between the experimental and calculated results is quite good over the entire  $H$  range. This is particularly true for the  $m(H)$  curves along the hard direction where magnetization occurs mainly by magnetization rotation, so the S-W model on which Eq. (1) is based is valid. However, a better fit was observed when the  $H_{\text{ex}}$  value was higher than 41 kA/m, the best fit being achieved at 43.4 kA/m, although the fitting results are not shown here. This means that the actual exchange coupling strength between IrMn and CoFe is higher than the bias field. This is obviously due to the interlayer coupling between free and pinned layers, as described in the previous section. It is seen from Eq. (1) that the difference between the actual exchange coupling strength and the bias field of the pinned layer switching is proportional to the product of  $H_{\text{int}}$  and  $M_f$ , specifically, the

Download English Version:

<https://daneshyari.com/en/article/8032874>

Download Persian Version:

<https://daneshyari.com/article/8032874>

[Daneshyari.com](https://daneshyari.com)